



UNCERTAINTY OF PRESSURE MEASUREMENT IN A SINGLE-BED ADSORBER

Mirosław Cezary Neska¹⁾, Tadeusz Andrzej Opara²⁾

- 1) *Lukasiewicz Research Network – Institute for Sustainable Technologies, K. Pułaskiego 6/10, 26-600 Radom, Poland*
(✉ miroslaw.neska@itee.lukasiewicz.gov.pl, +48 48 364 9354)
- 2) *Kazimierz Pułaski University of Technology and Humanities, Stasieckiego 54, 26-600 Radom, Poland,*
(t.opara@uthrad.pl)

Abstract

An adsorber in which sorption processes occur is one of the key components of an adsorption chiller. Precise real-time monitoring of and supervision over these processes are particularly important to ensure their proper execution. The article describes the experimental stand used for the measurement of the adsorber's operating parameters and analyses pressure measurement uncertainties, taking into account the impact of the temperature on the test system filled with the adsorbent in the form of silica gel, while concurrently considering the influence of other factors (e.g. the environment, the A/A, and A/D conversion, or data processing) on measurement uncertainties. A complex analysis of uncertainties was carried out, including the results of the statistical analysis of the measurement data obtained from long-term experimental tests of the object and the uncertainties of the pressure measuring chain by the type B method, involving the consideration of interactions between the system components and the temperature impact on the propagation of uncertainties. As part of the analysis, the characteristic stages of the data collection and processing operations related to the sampling rate and measurement intervals were separated. The article presents the prototype test stand and original pressure measurement system for the verification of a single-bed adsorber working below 10 hPa. The novel construction of a single-bed adsorber was used as a test object. Furthermore, in this paper, the developed algorithm of the research method implemented in the system was discussed and positively verified.

Keywords: measurement, uncertainty, adsorber, adsorbent bed, adsorption chiller.

© 2022 Polish Academy of Sciences. All rights reserved

1. Introduction

An adsorption chiller is a solution in which thermal energy from an external heat source must be supplied to force the circulation. Such solutions can be used in air conditioning systems [1–3], icemakers [4], or chillers [5, 6].

One of the key components of such a chiller is an adsorber in which an adsorbent bed is placed – this is where sorption processes occur. This component should have the following

features: tightness enabling the retention of vacuum; retention of adsorbent particles inside the adsorber; good heat exchange between the bed and the external thermal energy source [7]; and good adsorbate mass flow within the system [8,9]. These parameters have both direct and indirect impact on the coefficients of an adsorption chiller performance (COP and SCP), as described by Bahrehmand and Bahrami (2019) [10], who analyse a gravimetric large pressure jump test bed and a two-sorber composite bed and, among others, present the uncertainty of temperature and pressure measurements of the measuring components of the test stand.

This article describes the developed and built test stand with a single-bed adsorber and the novel measurement system, discussed below.

Pressure measurement in an adsorption system is of material importance due to the possibility to force internal sorption processes on the adsorbent material's surface at an assumed level of uncertainty. It is especially important when the pressure signal with the accepted tolerance is to be used for automatic control of sorption processes.

Sorption processes occurring in the bed include adsorbate adsorption and desorption. Sharafian *et al.* (2016) [11] describe adsorption and desorption processes in a zeolite-based bed for a waste heat-driven adsorption chiller for vehicle air conditioning applications with pressures ranging from 0.5 to 5.5 kPa. The article presents mathematical functions for the determination of the uncertainties of relative COP and SCP coefficients. Chen and Chua (2020) [12] suggest that pressure measurements be carried out in two points of a four-bed two-evaporator adsorption chiller, *i.e.* in the condenser and evaporator. To determine the measurement uncertainty, a mathematical formula was used to calculate the total uncertainty (e), as described by Moffat (1988) [13] and Adamczak (2015) [14]:

$$e = \pm \sqrt{\sum_{i=1}^{i=k} \left(\frac{\partial f}{\partial x_i} \right)^2 \cdot (\Delta x_i)^2}, \quad (1)$$

where: f the function of variables x_i ; Δx_i – total uncertainty of the parameters measured during the experiment; k – total number of measured values.

In the study, uncertainties of pressure and temperature measuring chain elements of a prototype single-bed test adsorber were determined. The literature review allowed an in-depth analysis of uncertainties that took into account the results of statistical tests and the uncertainty of the elements of the pressure and temperature measuring chain. The test methodology for the uncertainty calculation presented in the article based on the prototype solution in question can be used in an adsorption chiller, a single or multi-bed device [12, 15].

The article consists of eight sections. The original test stand with the prototype single-bed adsorber and the developed measurement system as well as the sources of uncertainty of the studied system are described in Sections 2 and 3, respectively. Section 4 presents the research method. In the next section, the dependence of the temperature effect on the tested system is determined. Section 6 contains the B type method uncertainty analysis. In the next two sections, the combined uncertainty of the measurement system was determined and the capability of the measurement system was analysed.

2. Test stand description

A developed prototype laboratory test stand was used for the verification of the results of pressure measurement in a single-bed adsorber (Fig. 1) and its variability over time. The study of a measuring system using porous materials and adsorption and desorption processes, as well as

the influence of environmental changes and pre-processing, are among the most important issues concerning the long-term stability of such a system [16].

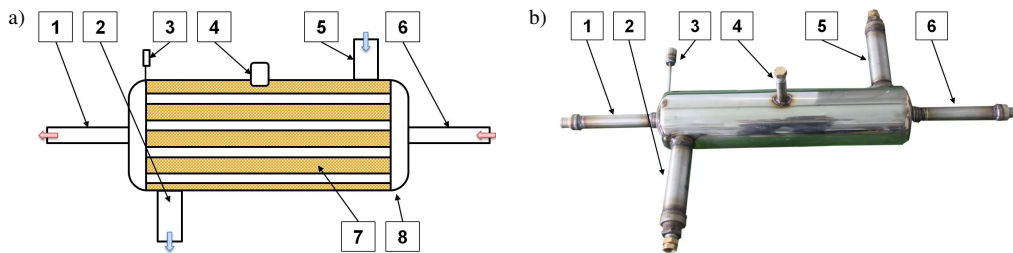


Fig. 1. Single-bed adsorber; a) simplified cross-section of the adsorber; b) steel housing view of the adsorber: 1 – outlet fluid circuit terminal; 2 – internal air circuit outlet connection; 3 – vent; 4 – measuring sensor connection; 5 – internal air circuit inlet connection; 6 – external fluid circuit inlet connection; 7 – silica gel bed; 8 – steel structure.

The discussed system consists of the test stand and the developed measurement system (Fig. 2). The stand is composed of the prototype single-bed adsorber (adsorber), vacuum pump that generates low pressure in the SB, air inlet/outlet shut-off valves, as well as sensors. The adsorber is a single-bed of 4.6 kg silica gel which is placed in a stainless steel housing built in the shape of a cylinder with the diameter of 130 mm and the length of 550 mm.

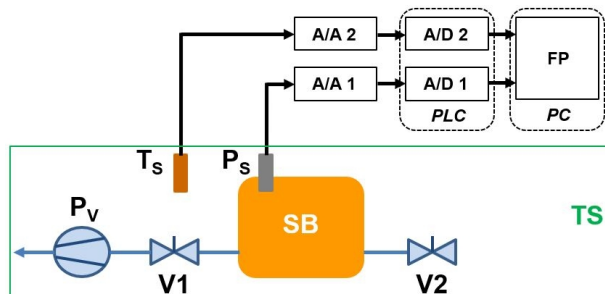


Fig. 2. Block diagram of the test stand (TS) with the measurement system; SB – single-bed adsorber, V – valve, P_V – vacuum pump, T_S – temperature sensor, P_S – pressure sensor, FP – further processing.

The measurement system is composed of a pressure sensor with an integrated A/A converter, a temperature sensor with an A/A converter, a PLC with built-in A/D modules, and a PC. The PLC and the PC are also equipped with the developed software for data processing.

The digital measurement signals generated in the system are transmitted to the PC in real-time via a Modbus Ethernet TCP/IP PC interface *for processing* (FP), recording, and visualisation

The presented test stand (Fig. 3) is designed to verify pressure in adsorbers at the prototyping stage. It does not include the testing of thermal and performance parameters of adsorption cooling systems. The development of this stand with additional functionalities, such as research on thermal and performance parameters of adsorption cooling systems, will be discussed in subsequent publications due to the complexity of the issues.

The pressure values indicated by the measuring head play two roles in the system: firstly, they are the input signal of the control system to determine the pressure level in the tested adsorber during its verification and, secondly, they are “true” values in the future static pressure characteristics determined for a given prototype adsorber. The input signals of a model of the

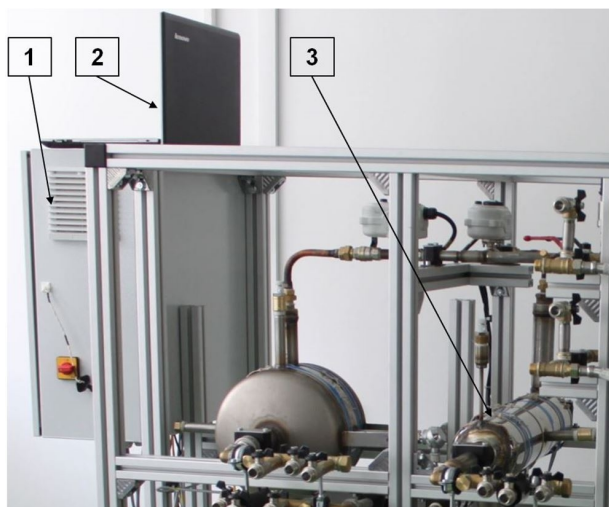


Fig. 3. View of the test stand for pressure verification in adsorbers; 1 – control and measurement system; 2 – PC; 3 – the SB tested.

measurement system (Fig. 4) are raw data, respectively: pressure ($X = P_S$) inside the adsorber, and the measured ambient temperature ($Y = T_S$).



Fig. 4. Model of the measurement system; X – pressure measured; Y – temperature measured; Z – result of the pressure measurement.

The output value of the model (Z) is the result of the pressure measurement with corrections related to the input values, which is described by the following formula: $Z = X + \delta X + Y + \delta Y$, where δ represents the pressure (δX) and temperature (δY) measurement errors respectively, which are discussed in detail below.

3. Sources of measurement uncertainty in the system

The main sources of errors in the analysed system (Fig. 2) include elements of the pressure and temperature measuring chains. The pressure measurement chain is equipped with a sensor with a built-in A/A converter (Table 1) and an A/D converter (Table 2) to which the analogue signal from the pressure sensor is transmitted. Once converted to the digital form, the signal is processed at the assumed sampling rate by the software installed on the PC and then archived.

The temperature measurement chain is equipped with a sensor with a built-in A/A converter (Table 3) that generates an analogue signal (in the form of voltage deviations) which, in turn, is transmitted to the A/D converter (Table 4). Once converted into the digital form, the signal is archived on the PC. Upon their identification, all potential error sources in the measuring system in question were analysed and presented in the form of the Ishikawa diagram (Fig. 5).

Table 1. Characteristics of the pressure sensor ($P_S + A/A1$).

Name and type	Element description and parameters
Pressure sensor: Cerabar PMC21, type: PMC21-AA1U2HBWBJA (Endress+Hauser) [17]	<ul style="list-style-type: none"> pressure measurement measuring range: 0÷100 kPa temperature of the agent: -25÷ + 100 V ambient temperature: -40÷ + 85°C; operation: +21÷ + 33°C relative humidity: 5÷80% ambient pressure: 860÷1060 hPa uncertainty in reference conditions with consideration of linearity, hysteresis, and repeatability: ±0.3% of the range total measurement uncertainty: 0.4% of value in the range of 1÷30 hPa long-term stability: ±0.2% of the range per annum power: 10÷30 VDC output: 4÷20 mA current output resolution: 1.6 µA mechanical connection: 1/2" thread; operating position of the measuring sensor: fixed (±1 relative to the level) separation membrane made of Al₂O₃, (Ceraphire®) with 99.9% purity

Table 2. Characteristics of the analogue and digital module of the pressure measuring chain (A/D1).

Name and type	Element description and parameters
A/C Modicon TM5 converter, PLC module, type: TM5SAI4L (Schneider Electric) [18]	<ul style="list-style-type: none"> digital resolution of the module: 12 bit input: 4÷20 mA module power: 20.4÷28.8 V DC input filter: low-pass 3rd order/cut-off frequency of 1 kHz input tolerance – maximum deviation at the ambient temperature of 25°C: < 0.08% of the measurement input tolerance – temperature drift: 0.009%/°C of the measurement tolerance – non-linearity: < 0.05% of the full scale (20 mA) resolution value: 4.883 µA

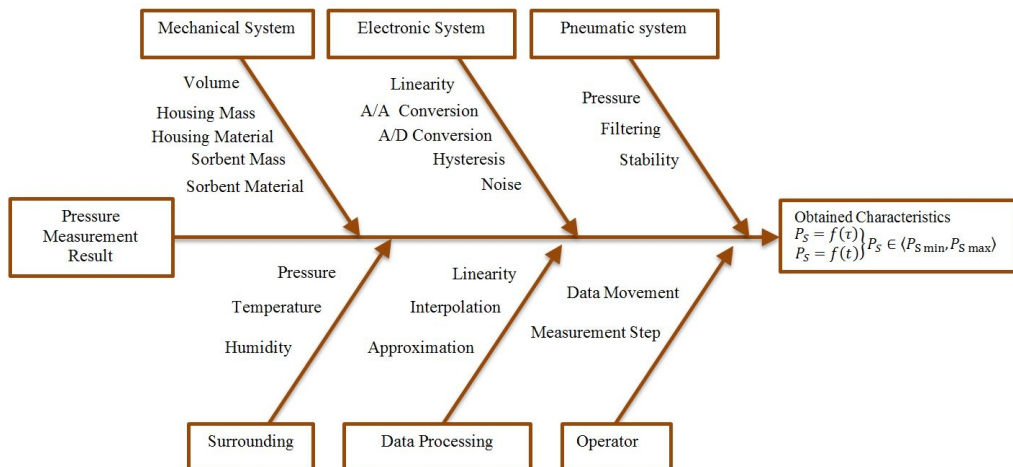


Fig. 5. Ishikawa diagram for the analysed test stand with a single-bed adsorber.

Table 3. Characteristics of the temperature converter ($T_S + A/A_2$).

Name and type	Element description and parameters
Temperature sensor, type: LM35CZ/NOPB (National Semiconductor Corporation) [19]	<ul style="list-style-type: none"> measuring range: $-40 \div +110^\circ\text{C}$ linearity: $+10 \text{ mV}/^\circ\text{C}$ total uncertainty: $\pm 0.4^\circ\text{C}$ ($+25^\circ\text{C}$) power: $4 \div 20 \text{ V DC}$ TO92, THT casing

Table 4. Characteristics of the analogue and digital module of the temperature measurement chain (A/D2).

Name and type	Element description and parameters
A/C Modicon TM5 converter, PLC module, type: TM5SAI4L (Schneider Electric) [18]	<ul style="list-style-type: none"> digital resolution of the module: 12 bit output: $-10 \div +10 \text{ V}$ module power: $20.4 \div 28.8 \text{ V DC}$ input impedance: $20 \text{ M}\Omega$ input filter: low-pass 3rd order/cut-off frequency of 1 kHz input tolerance – maximum deviation at ambient temperature of 25°C: $< 0.08\%$ of the measurement input tolerance – temperature drift: $0.006\%/^\circ\text{C}$ of the measurement input tolerance – non linearity: $< 0.025\%$ of the full scale (20 V DC) resolution value: 2.441 mV

4. Methodology and determination of measurement uncertainty

The developed algorithm (Fig. 6) of the research method for verification of pressure in the adsorber on the test stand is as follows. Firstly, for pressure of $P_{SIn} \approx 100 \text{ kPa}$, the air was pumped out from the single-bed adsorber. Next, the essential pumping stage started to obtain the set pressure level ($P_{SE} < 10 \text{ hPa}$), after which the valves (V_1, V_2) closed.

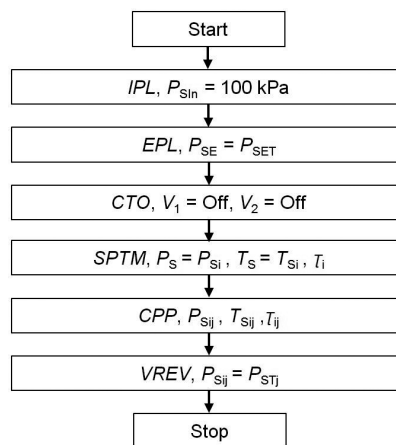


Fig. 6. Algorithm of the method of pressure verification of a test object; *IPL* – initial pumping of the air to the pressure level of 100 kPa; *EPL* – essential pumping of the air to the set level; *CTO* – closing the shutting valves controlling the inflow/outflow air to a test object; *SPTM* – starting pressure and temperature measurements; *CPP* – control of pressure parameters at selected intervals time; *VREV* – verification of the results with the expected values.

Then, a long-term pressure measurement was initiated to determine the pressure characteristics of the tested adsorber. As part of the test, the ambient temperature was also recorded. The long-term test allowed the estimation of the level of pressure changes in the *SB* – in total 14,048 pressure values were recorded. The pressure was measured at 30-second sampling steps for 117 hours and saved in a text file on the PC. In the next steps, the algorithm predicts control of the recorded pressure values at selected time intervals and verifies the results against the expected pressure values. The algorithm of the method ends after the verification of the results.

The tests allowed the determination of the variability of the measured value for pressure ranging between 5.0 and 6.3 hPa ($P_S < 10$ hPa). The registration of the entire process was divided into three time intervals (τ) (Fig. 7), *i.e.*: I – 2,450 samples; II – 6,326 samples; III – 5,272 samples. For each interval, a mathematical analysis of the data was performed, for the measurement start time: 5h (M_{5h}), 55h (M_{55h}), and 105h (M_{105h}). In each of these measurements (M_{5h} , M_{55h} , and M_{105h}), 30 samples lasting 15 minutes were taken to maintain the repeatability of the measurements. The results were subjected to statistical analysis to assess the pressure measurement uncertainty in the system. The minimum ($P_{S \min}$), maximum ($P_{S \max}$), and mean ($P_{S \text{mean}}$) values of individual intervals, as well as the ($P_{S \max} - P_{S \min}$) range, were determined. The results obtained are presented in Table 5. Due to the 0.4% uncertainty of the pressure measuring instrument used (Table 1), the analytical results were presented with an accuracy of 0.01.

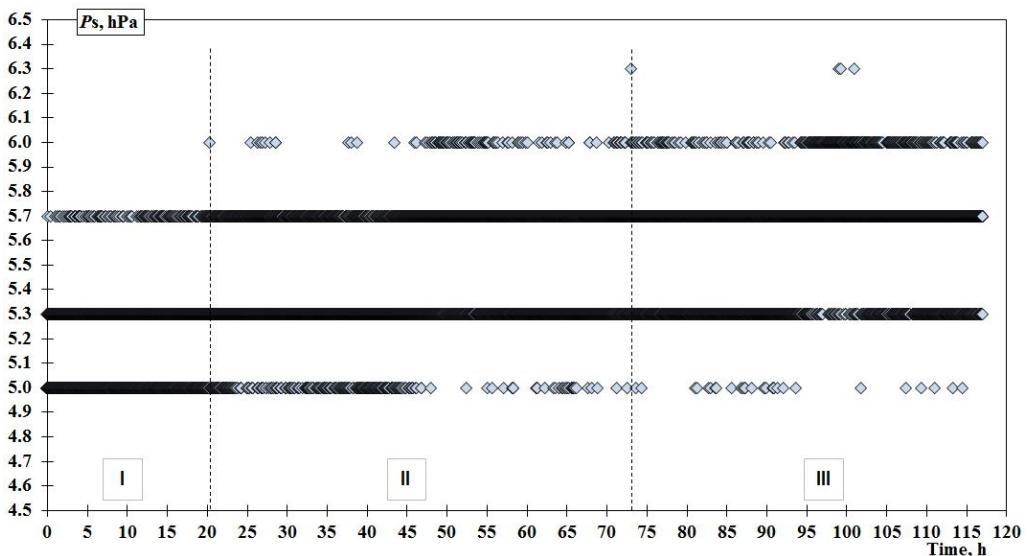


Fig. 7. Pressure values in the adsorber in low vacuum at intervals I, II, and III.

The analysis of the measurement uncertainty was based on the assumption that the data distributions obtained (M_{5h} , M_{55h} , and M_{105h}) are close to the normal distribution [20]. A sample histogram of similarity from the M_{55h} analysis with the normal distribution is shown in Fig. 8.

The standard experimental deviation $\sigma(P_S)$ of the sample for a single observation was defined. A histogram of the experimental observation variance for the three intervals is presented in Fig. 9. The mean calculated based on n individual observations is better determined through the mean experimental variance $\sigma_S(\bar{P}_S) = u_S = \sigma/\sqrt{n}$ [21].

Table 5. Summary of pressure values determined at different intervals M_{5h} , M_{55h} , and M_{105h} .

No.	P_{S5h} [hPa]	P_{S55h} [hPa]	P_{S105h} [hPa]
Mean	5.21	5.52	5.70
Max	5.70	6.00	6.00
Min	5.00	5.00	5.30
Max–Min	0.70	1.00	0.70
σ	0.17	0.26	0.17
$\sigma_S(\bar{P}_S) = u_S$ (for $n = 30$)	0.03	0.05	0.03
U_{95} (for $n = 30$)	0.06	0.10	0.06
$\bar{x} - 3\sigma$	5.12	5.38	5.61
$\bar{x} + 3\sigma$	5.31	5.67	5.79

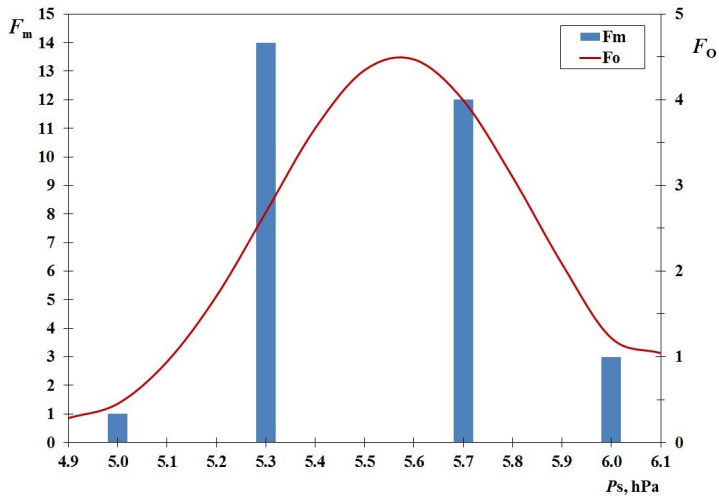
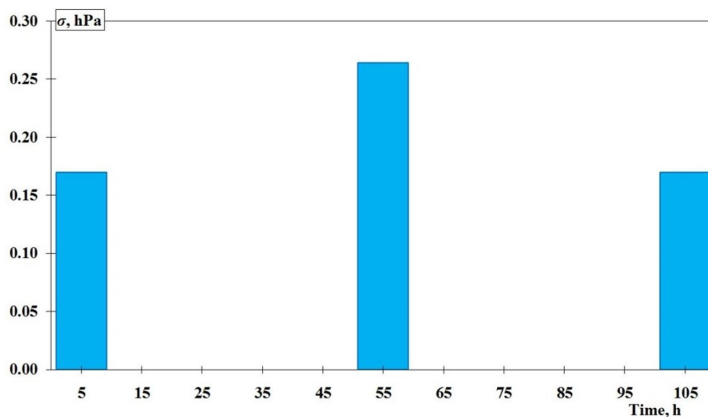
Fig. 8. Histogram presenting the distribution of pressure measurement results for the second interval and the measurement M_{55h} ; F_m – measured frequency; F_o – expected frequency for the normal distribution.

Fig. 9. Histogram of standard pressure measurement deviations for three intervals.

The expanded uncertainty for a series of repetitions can be calculated from the function $U_{95} = 1.960\sigma/\sqrt{n}$ [22]. The highest standard deviation was recorded for pressure measurement taken at 55 h (Fig. 10). For this interval, the maximum value of the expanded uncertainty stands at $U_{95 \max}$ (for $n = 30$) = 0.10 hPa.

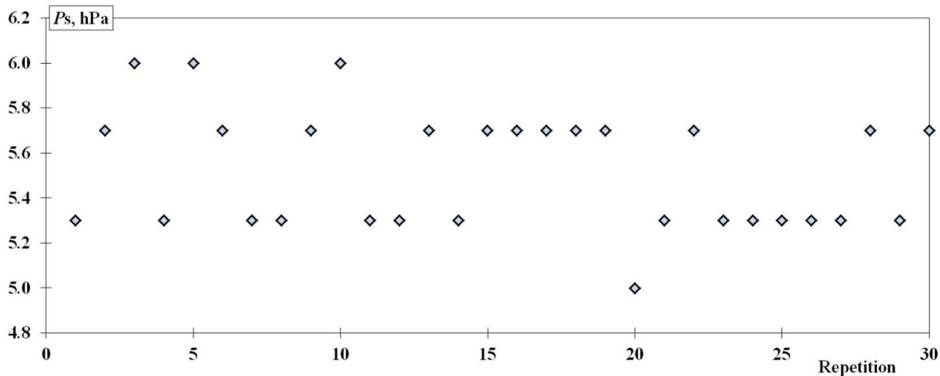


Fig. 10. Pressure measurement results for the second interval (55 h).

5. Temperature impact on pressure measurement

The data from air pressure measurements of the process under low vacuum conditions presented in the article were obtained for ambient temperatures listed in Table 6 and taken with an electronic temperature sensor (Table 3). Arithmetic means of pressure and ambient temperature for the measurements of M_{5h} , M_{55h} , and M_{105h} are determined based on the results of synchronous observations.

Table 6. Characteristic values of ambient temperature for the process.

No.	Mean	Max	Min	Max–Min
t [°C]	24.88	27.30	23.50	3.80

Temperature and pressure measurements were carried out simultaneously at an analogue sampling rate. Pressure measurements were taken in the adsorber without thermal insulation.

The main values and parameters of the ambient temperature obtained during the M_{55h} measurements are presented in Table 7.

Table 7. Summary of ambient temperature values at the time of the M_{55h} test.

No.	Mean	Max	Min	Max–Min	$\sigma_T(\bar{t}) = u_T(t)$	$U_{95}(t) = \delta Y$
t [°C]	25.01	25.30	24.80	0.50	0.03	0.06

As the measurements were carried out under repeatability conditions in 15-minute time intervals (M_{5h} , M_{55h} , and M_{105h}), there were slight fluctuations in temperature (at the level of 0.5°C) as well as pressure (Table 5), hence a linear model (Fig. 11) of the pressure-temperature relationship was adopted. The model was determined based on the data from the M_{55h} experiment, for which the highest value of the standard experimental deviation $\sigma(P_{55h})$ was obtained (Table 5).

M.C. Neska; T.A. Opara: UNCERTAINTY OF PRESSURE MEASUREMENT IN A SINGLE-BED ADSORBER

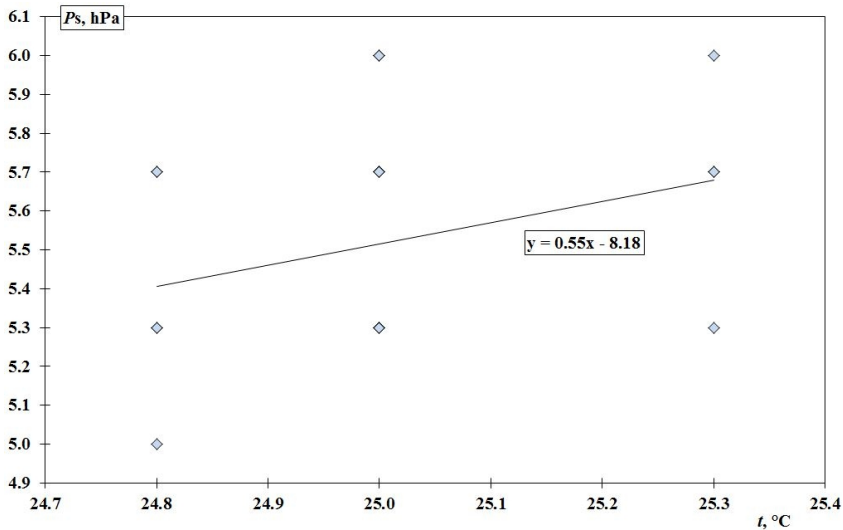


Fig. 11. Characteristic of the pressure-temperature relationship approximation for M_{55h} .

6. Effect of signal processing on the measurement result

When estimating the measurement uncertainty for the electronic pressure sensor, the individual components affecting the calculation of the measured value were determined (Fig. 12).

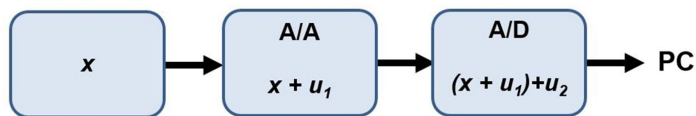


Fig. 12. Elements of the uncertainty propagation for the A/D conversion were based on [23].

In the analysed system, the x -value, as measured by the pressure sensor head, is subject to analogue processing, as part of which the obtained data are adjusted considering the A/A conversion uncertainty (u_1) and the A/D conversion uncertainty (u_2). The end measurement result obtained after the uncertainty analysis may be used directly as an input signal for the terminal controlling the process. It may also be further analysed and processed on the PC [24]. Individual uncertainties of the measuring chain determine the total uncertainty of the air pressure measuring chain in low vacuum conditions. The uncertainty of the standard pressure measurement $u_1(P_{AS}) = \Delta_{gr}P_{AS}/\sqrt{3}$ is calculated based on the A/A conversion limit deviation $\Delta_{gr}P_{AS}$ whose value is determined based on the specifications provided in Table 1 [25]. The A/D conversion resulted in an additional uncertainty, $u_2(M_{AD}) = \Delta_{gr}M_{AD}/\sqrt{3}$, determined by the limit deviation $\Delta_{gr}M_{AD} = (a \cdot x_{sr})/100 + n \cdot LSB$. Individual error components are determined based on specifications of the A/D converter (Table 4), the measurement error (a), and the converter resolution (LSB) [26]. The measurements were taken based on the resolution multiplication (n) equal to 1. The standard uncertainty values for the pressure measuring chain are listed in Table 8 and are related to the measurement of the M_{55h} , as the highest value (σP_{S55h}) was obtained in this measuring interval.

Table 8. Summary of standard uncertainties for the measurement chain.

x_{sr} [hPa]	$\Delta_{gr}P_{AS}$ [hPa]	$u_1(P_{AS})$ [hPa]	$\Delta_{gr}M_{AD}$ [hPa]	$u_2(M_{AD})$ [hPa]
5.52	0.12	0.07	0.31	0.18

7. Complex measurement uncertainty

The law of propagation of uncertainties [20] was applied to calculate the complex standard uncertainty of the pressure measurement $u_c(P_S)$ based on the Function (2). The formula was determined for $\partial P_S/\partial P_{AS} = 1$ and $\partial P_S/\partial M_{AD} = 1$. The $\partial P_S/\partial t$ coefficient function was calculated based on Characteristics 9 and the adopted approximate functional dependency $P_S = f(t)$. Expanded uncertainty $U_{95}(P_S) = \delta X$ was calculated for expansion coefficient k in (3) and the normal distribution was adopted as the probability distribution model of the measured quantity [25, 27].

$$u_c(P_S) = \sqrt{\left(\frac{\partial P_S}{\partial P_{AS}}\right)^2 u_1^2(P_{AS}) + \left(\frac{\partial P_S}{\partial M_{AD}}\right)^2 u_2^2(M_{AD}) + \left(\frac{\partial P_S}{\partial t}\right)^2 u_T^2(t) + u_S^2(P_S)}, \quad (2)$$

$$U_{95}(P_S) = k \cdot u_c(P_S). \quad (3)$$

The maximum expanded uncertainty was calculated for the measurement M_{55h} and its value was determined with the type B method and based on the frequency distribution [20] – is equal to 0.39 hPa for the coverage probability of 95%, which is the highest value of uncertainties estimated for the three variability intervals of the measurement data (Fig. 13). The error bars for individual intervals are presented with their linear approximation functions.

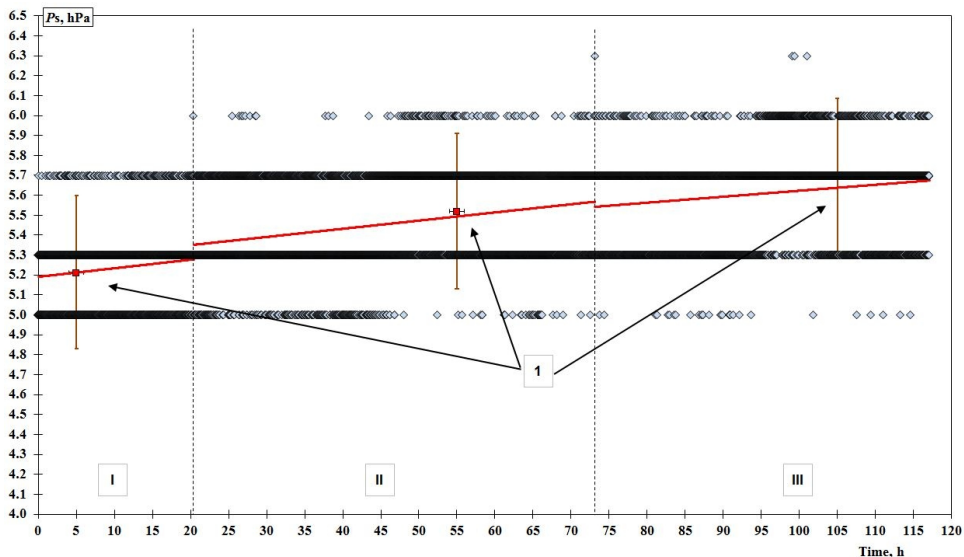


Fig. 13. Pressure-time relationship with the linear approximation functions and error bars; 1 – error bars and approximations for intervals I=III.

8. Analysis of the capabilities of the measuring system

New measuring systems and manufacturing processes are analysed for such attributes as *e.g.*, dispersion, centralisation, capability, repeatability, reproducibility, linearity, or stability [28–30]. The tests carried out with the developed measurement system described in the article are based on the repeatability (the third procedure – the special case of the *R&R* method) described in [31–34]. As part of the procedure, two measurements (each 25 minute-long) carried out at a 1-minute sampling rate were analysed. The results of the sample analysis for population II pressure measurements at 55 h are presented in Table 9.

Table 9. Summary of parameters for a standard deviation-based procedure.

$\bar{\Delta}$ [hPa]	s_{Δ} [hPa]	σ_{Δ} [hPa]	$EV_{0,99}$ [hPa]	$\%EV_{0,99}$ [%]
0.004	$7.4 \cdot 10^{-9}$	$5.2 \cdot 10^{-9}$	$2.7 \cdot 10^{-8}$	$1.1 \cdot 10^{-5}$

The dispersion (σ_{Δ}) of the measuring system and repeatability (*EV*) were calculated for the tolerance of the pressure sensor listed in Table 1. The relative repeatability value obtained for the tested measuring system falls within the $\%EV < 10\%$ range, which means that the system in question can be deemed as capable of proper operating. Taking $n_{\min} = 2$ as the sample size, the *upper control limit* (UCL) and the *lower control limit* (LCL) are obtained. The dispersion of the mean LC determines the distance of $\pm 3s_{\min}$ calculated for population II at 55 h of pressure measurement. Individual measurement values fall within the control lines in the natural process variability area (Fig. 14), as presented in the sample Shewhart chart [33]. The presented analysis is a part of the measurement system for verification of a test object but this system can as well constitute an element of an online control system, supervising manufacturing process run and efficiency work of a technical object.

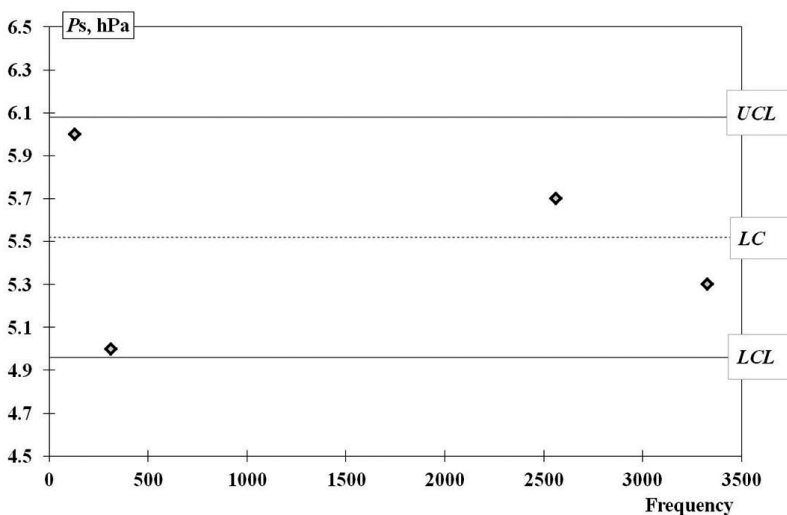


Fig. 14. Pressure measurement control chart (population II, 55 h interval).

9. Conclusions

The prototype test stand and the original pressure measurement system for an adsorber were developed. The algorithm of the research method implemented in the system was created and verified, obtaining positive results from its operation. As a test object, the original single-bed adsorber filled with silica gel was used.

The measurement uncertainty analysis confirmed that the assumptions and the architecture of the measuring system for pressure measurement in the single-bed adsorber were correct. Potential sources of uncertainty for the elements of the measuring chain were analysed and the main sources thereof were identified, which allowed the calculation of the uncertainty budget. The highest value of pressure sensor uncertainty for a random sample of n tests obtained through statistical analysis ($U_{95}(n = 30)$) totalled 0.095 hPa.

The propagation of uncertainties can be identified at successive stages of operation of the prototype measuring system in question. Further steps of the A/A and A/D measuring signal conversion process increase the frequency distribution-based uncertainty up to the maximum value of 0.39 hPa for the coverage probability of 95%. This change in value is influenced not only by the uncertainty of the individual signal processing steps but also by the ambient temperature. The estimated uncertainty value is satisfactory as it is below the assumed value of 10% of the minimum pressure sensor reading of 5.0 hPa. The positive verification of the entire system is also confirmed by the coefficient value ($\%EV < 10\%$).

The presented test stand with the pressure measurement system can be used for the verification of pressure in the adsorber at the adsorber prototyping stage or in its manufacturing run. Both the test stand and the pressure measurement system can also be used as potential sources of knowledge for the *statistical process control* (SPC) [34] during the manufacturing process of adsorption cooling systems.

The pressure measurement system, together with the algorithm, can also be used as one of the inspection elements of a more complex control system where the identification of the process approximation characteristics is required to determine the relationships necessary to develop a control algorithm [35, 36], or a calibration algorithm without synchronization signals [37]. As regards the adsorption chiller, these processes include forced adsorption and desorption phenomena.

References

- [1] Ramji, H. R., Leo, S. L., Tan, I. A. W., & Abdullah, M. O. (2014). Comparative study of three different adsorbent-adsorbate working pairs for a waste heat driven adsorption air conditioning system based on simulation. *IJRRAS*, 18(2), 109–121.
- [2] Tamainot-Telto, Z., Metcalf, S. J., & Critoph, R. E. (2009). Novel compact sorption generators for car air conditioning. *International Journal of Refrigeration*, 32(4), 727–733. <https://doi.org/10.1016/j.ijrefrig.2008.11.010>
- [3] Sur, A., & Das, R. K. (2017). Experimental investigation on waste heat driven activated carbon-methanol adsorption cooling system. *Journal of the Brazilian Society of Mechanical Sciences and Engineering*, 39, 2735–2746. <https://doi.org/10.1007/s40430-017-0792-y>
- [4] Pons, M., & Guilleminot, J. J. (1986). Design of an experimental solar-powered, solid-adsorption ice maker. *Journal of Solar Energy Engineering*, 108(4), 332–337. <https://doi.org/10.1115/1.3268115>

- [5] Szyc, M., & Nowak, W. (2014). Operation of an adsorption chiller in different cycle time conditions. *Chemical and Process Engineering*, 35(1), 109–119. <https://doi.org/10.2478/cpe-2014-0008>
- [6] Sur, A., Das, R. K., & Sah, R. P. (2018). Influence of initial bed temperature on bed performance of an adsorption refrigeration system. *Thermal Science*, 22(6A), 2583–2595. <https://doi.org/10.2298/TSCI160108254S>
- [7] Mohammed, R. H., Mesalhy, O., Elsayed, M. L., Su, M., & Chow, L. C. (2018). Revisiting the adsorption equilibrium equations of silica-gel/water for adsorption cooling applications. *International Journal of Refrigeration*, 86, 40–47. <https://doi.org/10.1016/j.ijrefrig.2017.10.038>
- [8] Kaushik, S. C., & Mahesh, A. (2013, April 16–20). Solar adsorption cooling system: some materials and collectors aspects. *SOLAR 2013 Conference Including Proceedings of 42nd ASES Annual Conference Proceedings of 38th National Passive Solar Conference*. North America.
- [9] Sah, R. P., Choudhury, B., Das, R. K., & Sur, A. (2017). An overview of modelling techniques employed for performance simulation of low-grade heat operated adsorption cooling systems. *Renewable and Sustainable Energy Reviews*, 74, 364–376. <https://dx.doi.org/10.1016/j.rser.2017.02.062>
- [10] Bahrehmand, H., & Bahrami, M. (2019). An analytical design tool for sorber bed heat exchangers of sorption cooling systems. *International Journal of Refrigeration*, 100, 368–379. <https://doi.org/10.1016/j.ijrefrig.2019.02.003>
- [11] Sharafian, A., Mehr, S. M. N., Thimmaiah, P. C., Huttema, W., & Bahrami, M. (2016). Effects of adsorbent mass and number of adsorber beds on the performance of a waste heat-driven adsorption cooling system for vehicle air conditioning applications. *Energy*, 112, 481–493. <http://dx.doi.org/10.1016/j.energy.2016.06.099>
- [12] Chen, W. D., & Chua, K. J. (2020). Parameter analysis and energy optimization of a four-bed, two-evaporator adsorption system. *Applied Energy*, 265(114842), 1–16. <https://doi.org/10.1016/j.apenergy.2020.114842>
- [13] Moffat, R. J. (1988). Describing the uncertainties in experimental results. *Experimental Thermal and Fluid Science*, 1(1), 3–17. [https://doi.org/10.1016/0894-1777\(88\)90043-X](https://doi.org/10.1016/0894-1777(88)90043-X)
- [14] Adamczak, S., Bochnia, J., & Kaczmarska, B. (2015). An analysis of tensile test results to assess the innovation risk for an additive manufacturing technology. *Metrology and Measurement Systems*, 22(1), 127–138. <https://doi.org/10.1515/mms-2015-0015>
- [15] Pan, Q., Peng, J., & Wang, R. (2019). Experimental study of an adsorption chiller for extra low temperature waste heat utilization. *Applied Thermal Engineering*, 163(114341), 1–8. <https://doi.org/10.1016/j.applthermaleng.2019.114341>
- [16] Chludziński, T., & Kwiatkowski, A. (2020). Exhaled breath analysis by resistive gas sensors. *Metrology and Measurement Systems*, 27(1), 81–89. <https://doi.org/10.24425/mms.2020.131718>
- [17] Endress+Hauser. (2017). *Cerabar PMC11, PMC21, PMP11, PMP21 Process pressure measurement* [Technical information TI01133P/00/EN/05.17 71353705]. https://portal.endress.com/wa001/dla/5001041/2232/000/04/TI01133PEN_0517.pdf
- [18] Schneider Electric. (2018). *Modicon TM5 Analog I/O Modules Hardware Guide*. [Technical information 03/2018, EIO0000000450.04]. https://download.schneider-electric.com/files?p_enDocType=User+guide&p_File_Name=EIO0000000450.06.pdf&p_Doc_Ref=EIO0000000450
- [19] National Semiconductor Corporation. (2000). *LM35 Precision Centigrade Temperature Sensors*. [Datasheet DS005516]. https://www.digchip.com/datasheets/download_datasheet.php?id=513966&part-number=LM35DZ

- [20] Joint Committee for Guides in Metrology. (2008). *Evaluation of measurement data – Guide to the expression of uncertainty in measurement* (JCGM 100:2008). http://www.bipm.org/utlis/common/documents/jcgm/JCGM_100_2008_E.pdf
- [21] Domanska, A. (2011). Uncertainty of the Analog to Digital Conversion Result. *Measurement Uncertainty, Theory and Practice*, Fotowicz, P., (Ed.), GUM, 22–31. (in Polish)
- [22] Neska, M., & Majcher, A. (2014). Estimation of the uncertainty of measurement in a two-channel system for tests on the intensity of infrared radiation. *Problemy Eksploatacji – Maintenance Problems*, 3, 45–55.
- [23] Jermak, C. J., Jakubowicz, M., Derezynski, J., & Rucki, M. (2017). Uncertainty of the Air Gauge Test Rig. *International Journal of Precision Engineering And Manufacturing*, 18(4), 479–485. <https://doi.org/10.1007/s12541-017-0058-8>
- [24] Neska, M., & Majcher, A. (2015). System for automatic web guiding for roll-to-roll machine working in a start-stop mode. *Solid State Phenomena*, 223, 374–382. <https://doi.org/10.4028/www.scientific.net/SSP.223.374>
- [25] EA European Accreditation. (2021). *Evaluation of the Uncertainty of Measurement in Calibration. European Co-operation for Accreditation* (Publication References EA-4/02 M:2021). <https://european-accreditation.org/wp-content/uploads/2018/10/EA-4-02.pdf>
- [26] Nuccio, S., & Spataro, C. (2008, Sep. 22-24). Figures of Merit for Analog-to-Digital Converters: The Optimal Set for the Uncertainty Evaluation. *13th Workshop on ADC Modelling and Testing*. Italy.
- [27] Dzwonkowski, & A., Swędrowski, L. (2012). Uncertainty analysis of measuring system for instantaneous power research. *Metrology and Measurement Systems*, 19(3), 573–582. <https://doi.org/10.2478/v10178-012-0050-7>
- [28] Bullock, R., & Deckro, R. (2006). Foundations for system measurement. *Measurement*, 39(8), 701–709. <https://doi.org/10.1016/j.measurement.2006.03.009>
- [29] Jermak, C. J., Jakubowicz, M., Dereżyński, J., & Rucki, M. (2016). Air Gauge Characteristics Linearity Improvement. *Journal of Control Science and Engineering*, 8701238, 1–7. <https://doi.org/10.1155/2016/8701238>
- [30] Jermak, C. J., & Rucki, M. (2016). Static characteristics of air gauges applied in the roundness assessment. *Metrology and Measurement Systems*, 23(1), 85–96. <https://doi.org/10.1515/mms-2016-0009>
- [31] Sałaciński, T. (2012). Analysis of tools and measurement systems capabilities. *Inżynieria Maszyn*. 2(17), 74-83. (in Polish)
- [32] Rucki, M., Barisic, & B., Szalay, T. (2008). Analysis of air gage inaccuracy caused by flow instability. *Measurement*, 41(6), 655–661. <https://doi.org/10.1016/j.measurement.2007.10.001>
- [33] Dietrich, E., & Schulze, A. (2010). *Statistical Procedures for Machine and Process Qualification*. Hanser Fachbuchverlag.
- [34] Sałaciński, T. (2015). *SPC – Statistical Process Control*. The Warsaw University of Technology Publishing House.
- [35] Neska, M., Majcher, A., & Przybylski, J. (2013). Control software for a reconfigurable control system for a set of testing devices. *Problemy Eksploatacji – Maintenance Problems*, (2), 57–68.
- [36] Neska, M. (2015). Measurement system for IR absorption. *Problemy Eksploatacji – Maintenance Problems*, (1), 91–100.
- [37] Cheng, H. M., Huang, Q. F., Ji, F., Xu, Q., Liu, J., & Tian, Z. Q. (2018). System for calibrating analogue merging units in absence of synchronization signals. *Metrology and Measurement Systems*, 25(1), 129–138. <https://doi.org/10.24425/118169>

M.C. Neska; T.A. Opara: UNCERTAINTY OF PRESSURE MEASUREMENT IN A SINGLE-BED ADSORBER



Mirosław Cezary Neska, Specialist in the Control Systems Research Group/Technical Manager in the Control Systems Laboratory in the Lukaszewicz Research Network – Institute for Sustainable Technologies, Radom, Poland (since 2007); Ph.D. student at the Kazimierz Pulaski University of Technology and Humanities in Radom, Poland. He received the M.Sc. degree from the AGH University of Science and Technology, Krakow, Poland, and the Eng. degree from the Kazimierz Pulaski University of Technology in

Radom, Poland. He won a scholarship to attend the ICAM Nantes Technical University, France, as part of the Socrates/Erasmus program. He completed an internship as a production-quality engineer in CAILLAU (2006), Romorantin, France. He has authored or co-authored over 30 scientific articles published in Polish and international journals and participated in over 20 Polish and international conferences. His professional interests include control systems, energy systems, renewable energy, programmable systems, measurement systems, metrology, computer process control, and electromagnetic compatibility.



Tadeusz Andrzej Opara received Ph.D. and D.Sc. from the Military University of Technology, Warsaw, Poland, in 1982 and 1997. He received the title of Professor at the Rzeszów University of Technology in 2012. He is currently Full Professor at the Faculty of Mechanical Engineering of the University of Technology and Humanities in Radom. He has authored 2 books and over 70 journal publications. His interests include the physical properties

of liquid crystals, diffraction methods for studying the spray spectrum of fuel aerosols, composite ablative materials, posturography studies of pilots, and thermodynamic issues.